

Comprehensive analysis of human microRNA-mRNA interactome

1 **Olga Plotnikova^{1,*}, Ancha Baranova^{2,3}, Mikhail Skoblov^{2,4}**

2 ¹Laboratory of functional genome analysis, Moscow Institute of Physics and Technology, Moscow,
3 Russia

4 ²Laboratory of functional genomics, Research Centre for Medical Genetics, Moscow, Russia

5 ³School of Systems Biology, George Mason University, Fairfax, VA, USA

6 ⁴School of Biomedicine, Far Eastern Federal University, Vladivostok, Russia

7

8 *** Correspondence:**

9 Olga Plotnikova

10 plotnikova@phystech.edu

11 **Keywords: microRNA, regulation of gene expression, microRNA-mRNA interactions, microRNA**
12 **binding sites, miRNA-target RNA duplexes, web tool for searching microRNA-binding regions**

13

14 **Abstract**

15 MicroRNAs play a key role in the regulation of gene expression. A majority of microRNA-mRNA
16 interactions remain unidentified. Despite extensive research, our ability to predict human
17 microRNA-mRNA interactions using computational algorithms remains limited by a complexity of
18 the models for non-canonical interactions, and an abundance of false positive results.

19 Here we present the landscape of microRNA-mRNA human interactions, which we derived from
20 comprehensive analysis of datasets describing direct microRNA-mRNA interactions experimentally
21 defined in HEK293 and Huh7.5 cell lines, along with other available microRNA and mRNA expression
22 data. We have also established a collection of reliable microRNA binding regions that we
23 systematically extracted in course of analysis of 79 CLIP datasets, which is available at
24 <http://score.generesearch.ru/services/mirna/>.

25 While only 1-2% of human genes interact with microRNAs, some RNAs display a substantial sponge
26 effect, which is specific to the cell line of study. Some microRNAs are expressed at a very high level,
27 while interacting with only a few mRNAs, thus, indeed, serving as specific gene expression
28 regulators. Other miRNAs might be expressed at relatively low levels, and interact with many
29 mRNAs. Some of the microRNAs might switch between these two classes, depending on cellular
30 context. Results of our study provide an initial resolution into the complex patterns of human
31 microRNA-mRNA interactions.

32 **1 Introduction**

33 MicroRNAs are small noncoding RNAs that associate with Argonaute (*AGO*) protein to form a
34 silencing complex, which then regulates a gene expression (Jonas and Izaurralde, 2015). MicroRNAs
35 accomplish essential post-transcriptional regulatory step of gene expression regulation through
36 either the degradation of a transcript or the inhibition of translation, and are involved in key cellular
37 processes, such as apoptosis, proliferation or differentiation (He and Hannon, 2004). Hence, the
38 dysregulation of microRNAs could result in the development of a disease or in a malignant
39 transformation (Weiss and Ito, 2017). According to some estimates, nearly all mature sequences of
40 coding transcripts contain potential sites for microRNA regulation (Bartel, 2004; Friedman et al.,
41 2009).

42 Human genome encodes approximately 2600 mature microRNAs (miRBase v.22) and, according to
43 GENCODE data (v.29), more than 200 thousands of transcripts, including isoforms with slight
44 variations. A particular microRNA may target many different mRNAs (Selbach et al., 2008); a
45 particular messenger RNA may bind to a variety of microRNAs, either simultaneously or in context-
46 dependent fashion (Uhlmann et al., 2012). Notably, within some messenger RNAs, the target
47 regions for particular microRNAs cluster together, resulting in the cooperative repression effect
48 (Grimson et al., 2007; Sætrom et al., 2007). The mapping of microRNA-mRNA interactions is far
49 from being complete due to the recognized challenges of computational prediction of mRNA-
50 microRNA interactions.

51 In our previous study, we showed that the outputs generated by commonly used microRNA-mRNA
52 interactions predicting software differ from each other substantially, while failing correctly pinpoint
53 microRNA-binding regions identified in wet lab experiments (Plotnikova and Skoblov, 2018).
54 Nowadays, many tools for the prediction microRNA-mRNA interactions are in development, all with
55 different underlying algorithms (Riffo-Campos et al., 2016; Gumienny and Zavolan, 2015; Lu and
56 Leslie, 2016; Agarwal et al., 2015;). Among most advanced algorithms we should highlight the ones
57 taking into account expression levels of both the microRNAs and their targets. Notably, the changes
58 in expression of microRNA may also affect expression levels of other, non-target mRNAs, for
59 example, due miRNA targeting of their upstream regulators. Consequently, newer, more
60 comprehensive approaches, like miRImpact (Artcibasova et al., 2016), PanMiRa (Li and Zhang,
61 2014), and ProMiSe (Li et al., 2014), aim at explaining complex phenotypes by performing analysis
62 of each microRNAs along with its direct and indirect targets.

63 The experimental identification of direct microRNA targets remains a crucial step in attaining good
64 prediction results. There are two main groups of the experimental approaches for a direct
65 identification of microRNA-mRNA interactions. The first approach relies on a construction of
66 reporter gene assays and one-by-one evaluation of possible interactions between the microRNA
67 and its cognate mRNA region of interest through measuring the activity of the reporter (Steinkraus
68 et al., 2016). Another group of techniques comprises involves a coupling of a cross-linking with

69 immunoprecipitation (CLIP); this group represented by variety of the protocols including PAR-CLIP,
70 iCLIP, HITS-CLIP, and others (Steinkraus et al., 2016; Licatalosi et al., 2008). CLIP group of methods
71 identifies the microRNA binding regions in target mRNAs only, while information about pairing of a
72 particular microRNA with a particular mRNA region remains obscure.

73 There are two modifications of AGO-CLIP based technology developed specifically for identifying
74 microRNAs ligated to their endogenous mRNA targets as part of chimeric molecules. To date,
75 evaluations of microRNA-mRNA interactomes by these two technologies utilized only two human
76 cell lines. Helwak and colleagues applied so-called cross-linking ligation and sequencing of hybrids,
77 or CLASH, to HEK293 cell line, retrieving more than 18,000 high-confidence microRNA-mRNA
78 interactions (Helwak et al., 2013). Later, Moore and colleagues used another variety of AGO-CLIP
79 termed CLEAR (covalent ligation of endogenous Argonaute-bound RNAs)-CLIP for the study of
80 microRNA-interactome in Huh7.5 cell (Moore et al., 2015). CLASH and CLEAR-CLIP techniques
81 closely resemble each other, with the only difference that CLASH protocol employs HEK293 cell line
82 over-expressed AGO1, while CLEAR-CLIP targets endogenous AGO allowing experimenting with any
83 cell line. Thus, CLEAR-CLIP does not require full denaturation of AGO and involves a single
84 purification step. It is of note that both publications cited above concentrated on the development
85 of the experimental protocol and subsequent evaluation of the technical aspects of analytic
86 procedure, rather than on extracting biological insights from the data collected.

87 We aggregated various experimental data on human miRNA-mRNA interactions, and analyzed
88 them. First, we investigate how expression levels of microRNAs and their cognate mRNAs correlate,
89 and if the behavior of miRNA-mRNA pairs depends on a cell line context. In order to do this, we
90 analyzed together (i) sequences and abundance of microRNA and their target mRNAs in CLASH
91 dataset for HEK293 cell line and in CLEA-CLIP dataset for Huh7.5 cell line and (ii) expression level of
92 microRNAs and RNAs in HEK293 and in Huh7.5 cell lines. Second, we attempted an identification of
93 a credible, experimentally confirmed microRNA binding regions in CLASH/ CLEAR-CLIP datasets and
94 in 79 additional CLIP datasets.

95

96 **2 Materials and Methods**

97 **2.1 microRNA-mRNA interactions**

98 microRNA-mRNA interactome data were extracted from published CLASH (Helwak et al., 2013) and
99 CLEAR-CLIP (Moore et al., 2015) studies. Using Ensemble API, the coordinates of microRNA – mRNA
100 interacting regions were transformed into genome coordinates. In total, we revealed 18,478
101 microRNA-mRNA interactions in 22,030 genome regions. For a total of 36 interactions, the
102 transforming of their coordinates failed. We used LiftOver to transform CLEAR-CLIP interactome
103 data from hg18 genome version into hg19. wAnnovar (Wang et al., 2010; Yang and Wang, 2015)

104 was used to annotate genomic regions (CDS, 3'UTR, 5'UTR, intronic, intergenic, etc). To estimate the
105 expected overlap between CLASH and CLEAR-CLIP like datasets we used a custom python script.

106 **2.2 mRNA expression**

107 Publicly available RNA-seq datasets GSE68611 (Murakawa et al., 2015) and GSE64677 (Luna et al.,
108 2015) were used for extracting and examining gene sets expressed in HEK293 and Huh7.5 cell lines.
109 Each of these datasets includes two biological replicates. Initial quality control of sequencing
110 outputs was performed using FastQC. Next, we used kallisto (Bray et al., 2016) to map raw reads to
111 the human reference transcript sequences (GENCODE, 28 version).

112 First, in each experiment, we calculated the gene expression levels as the sum of expression levels
113 for individual gene transcripts. Second, we took the mean value for each gene between two
114 processed datasets in each of the two cell lines. Finally, we kept only genes that had expression
115 more or equal to 1 tpm as total value and that had expression level of at the level at least 1 tpm in
116 one of the two experiments.

117 To reveal an amount of interactions with microRNAs for genes, we used CLASH and CLEAR-CLIP
118 datasets for HEK293 and Huh7.5 cell lines, respectively.

119 Gene functions were interpreted using PANTHER toolkit Version 12.0
120 (<http://www.pantherdb.org/tools>). We used InteractiVenn tool (Heberle et al., 2015) to create Venn
121 diagrams in our analysis.

122 **2.3 microRNA expression**

123 We downloaded microRNA expression data from the GEO database: two experimental replicates for
124 HEK293 cell line (GSE75136 (Wissink et al., 2016)) and three experimental replicates for Huh7.5 cell
125 line (GSE74014 (Bandiera et al., 2016)). The correlations of experimental results obtained in two cell
126 lines were calculated using the Spearman's procedure. We used the R package "DeSeq2" to
127 normalize microRNA expression. MicroRNA was considered as expressed if it had expression more
128 than 3 counts.

129 CLASH and CLEAR-CLIP datasets were used to calculate the amount of interactions for each
130 microRNAs. The correlation of the amounts of interactions formed by microRNAs and their
131 expression levels were estimated using the Spearman correlation coefficient.

132 In order to calculate a conservative phyloP score for all microRNAs we downloaded the coordinates
133 of the mature microRNAs from miRBase (Kozomara and Griffiths-Jones, 2013) (release 22,
134 coordinates corresponded to the GRCh38 human reference genome). Next, we used UCSC table
135 browser (Karolchik et al., 2004) to obtain phyloP conservative values across 20 vertebrates for all
136 mature microRNAs. For each group of microRNAs, the mean value between the phyloP scores was
137 calculated.

138 **2.4 CLIP-data**

139 We collected 79 CLIP datasets (Supplementary Table 3) from the POSTAR database (Hu et al., 2016)
140 that were initially preprocessed by unified procedures: PAR-CLIP datasets (N = 18) by PARalyzer
141 (Corcoran et al., 2011) method and HITS-CLIP datasets (N = 61) by CIMS (Moore et al., 2014)
142 method. We used python to analyze all microRNA binding regions from CLIP datasets together with
143 microRNA-mRNA interactions from CLASH and CLEAR-CLIP. In total, all regions were merged in six
144 million nucleotides and each position was characterized by the following parameters: list of
145 supported experiments (GEO GSM ID), their corresponding cell lines and list of interacted
146 microRNAs (if accessible). We used wAnnovar to annotate genes and their parts (CDS, 3'UTR, 5'UTR,
147 intronic, etc).

148 **2.5 microRNA binding regions**

149 Our analysis of CLIPs, CLASH, and CLEAR-CLIP revealed 156 thousand regions. We used a custom
150 python script to select experimentally confirmed microRNA binding regions (Exp-MiBR). Exp-MiBR
151 was defined as a region that had a subsequence of length $L=10$, whereas each nucleotide (position)
152 in this subsequence had been supported by at least $n=2$ different datasets or chimeras. We
153 estimated the amount of Exp-MiBRs for all combination of length and amount of supported
154 datasets/chimeras in ranges: $L=1-25$ and $n=1-10$ (Supplementary Table 5).

155 **2.6 Exp-MiBRs application**

156 We characterized each Exp-MiBR (total amount = 46805) by the following parameters: gene
157 information; amount and list of supported experiments (GEO GSM ID) and their corresponding cell
158 lines; list of interacted microRNAs (if accessible).

159 Besides that all the Exp-MiBRs with the corresponded information are available as Supplementary
160 Table 4, we also provide an open-access web tool via <http://score.generesearch.ru/services/mirna>.
161 As input, the tool requires any VCF file (v4.0 or 4.1), no more than 20MB or a single (point) genome
162 coordinate. The file or coordinate could be recorded in human genome assembly version 38 or 19.

163 **2.7 Web tool for searching Exp-MiBRs**

164 All microRNA binding regions identified as experimentally confirmed (Exp-MiBR) and reported in
165 this paper (Supplementary Table 4) may be searched by a web tool available online:
166 <http://score.generesearch.ru/services/mirna/>.

167

168 **3 Results**

169 **3.1 Comparison of high-throughput microRNA-mRNA interactions from CLASH and CLEAR-CLIP** 170 **datasets**

171 First, we compared the sets of microRNA-mRNA interactions retrieved in HEK293 and in Huh7.5 by
172 CLASH (Helwak et al., 2013) and CLEAR-CLIP (Moore et al., 2015) protocol, respectively. Although
173 CLASH and CLEAR-CLIP techniques are somewhat similar, CLEAR-CLIP study (N=32,170) revealed
174 almost two times more interactions than CLASH study (N=18,478). One of the reasons for this may
175 be due to the differences in the data processing procedures. While CLASH sequences were aligned
176 to the mature transcriptome, CLEAR-CLIP data have been mapped to human genome. Because of
177 that, CLEAR-CLIP technique was capable to highlight additional interaction sites located in the
178 introns and the intergenic regions (~70% of all interactions).

179 To enable the comparison, we focused our analysis on miRNA binding regions residing within the
180 mature transcriptome. Because of that, CLEAR-CLIP dataset was limited to about one-third of its
181 entries (n=10,032). Further analysis estimated that approximately 2-3% of the total length of all
182 expressed protein-coding transcripts serve as a target for one or another microRNAs in either CLASH
183 or CLEAR-CLIP datasets. In addition, in both datasets, the microRNA binding regions had similar
184 distribution by mRNA regions (3' UTR, CDS, 5' UTR), and to the distribution of the mRNA parts
185 present in GENCODE (Figure 1A). Thus, the datasets generated by CLASH and CLEAR-CLIP techniques
186 are comparable.

187 Comparison of these two studies revealed approximately one thousand common binding regions
188 found both in a set of eighteen thousand interactions from CLASH and in a set of ten thousand
189 interactions from CLEAR-CLIP. To evaluate if this overlap reflect biological phenomenon rather than
190 statistical fluke, we performed computational simulation of CLASH and CLEAR-CLIP interactions in
191 transcripts expressed in HEK293 (N = 7,299) and Huh7.5 (N = 4,977), respectively. For these cell
192 lines, a common set of expressed mRNAs (n = 3,044) was reduced to a set of randomly selected
193 nucleotide fragments with the size distribution matching that for nucleotide fragments of CLASH
194 and CLEAR-CLIP, then we analyzed these sets of sequences for overlap. After five independent runs
195 with randomly selected fragments of matching size distribution, we detected, on average, 7.4 +/-
196 1.3 interactions with an average length of overlapped segments at 14 nt +/- 6.7 nt. Among these
197 interactions, only a fraction had the length of overlap of more than 20 nt (5.0 +/- 2.5). In the
198 experimentally obtained CLASH and CLEAR-CLIP datasets, we detected 1,153 common miRNA-
199 mRNA interactions, built upon combinations of 933 fragments interacting in CLASH and 944
200 fragments interacting in CLEAR-CLIP. Average length of experimentally obtained interaction was at
201 37.2 nt +/- 19.4 nt. Eight hundred and sixty seven interactions which were common for both
202 datasets had the length of overlap of more than 20 nt, with an average length of 45.8 nt +/- 13.9 nt.
203 Therefore, the characteristics of experimentally detected patterns of miRNA-mRNA interactions
204 differ from that of interactions generated by simulation of random events (P < 0.0001).

205 To investigate whether the low degree of the overlap between miRNA-mRNA interactions
206 registered in CLASH and CLEAR-CLIP datasets could be due to low degree of the overlap between
207 HEK293 and Huh7.5 transcriptomes, expression data collected from these two cell lines were
208 downloaded from GEO repository and analyzed. While about half of expressed microRNAs were

209 common for both these cell lines (Figure 1C), overall difference in expression patterns of HEK293
210 and Huh7.5 cells (Figure 1B) was clearly evident. To find out if cell-specific differences in microRNA-
211 mRNA interactomes are due to cell-specific environment, the relationships between the levels of
212 expression for individual miRNAs and their targets as well as the patterns of interactions for each
213 mRNAs and miRNAs in the both cell lines were investigated in details.

214

215 **3.2 Expression analysis of microRNA-mRNA interactome**

216 **3.2.1 mRNA expression analysis**

217 To investigate the degree to which cell-specific levels of transcripts depend on respective
218 microRNAs, we compared expression levels of each gene in HEK293 and Huh7.5 cell lines, then
219 cross-compared them to sets of experimentally detected microRNA interactions. HEK293 and
220 Huh7.5 cell lines express a total of 15,8k and 14,5k genes, respectively. In each of these two cell
221 lines, approximately 6.9k genes interacted with one or more microRNAs (Supplementary Fig. 1). Our
222 analysis pinpointed 1-2% of mRNAs with confirmed interactions and no expression detected in the
223 corresponding cell line. It is possible that these mRNAs have been detected as chimeric reads
224 resulting from their protection by AGO protein from Ribonucleases. Below, we will describe a few
225 microRNAs that were detected only as a part of chimeras.

226 In each of these cell lines, a majority of expressed mRNAs (57-59%) did not interact with any
227 microRNA (Figure 2AB). In CLASH and CLEAR-CLIP datasets, there were 215 and 333 high-
228 interacting mRNAs, respectively, with nine or more miRNA interactions for each.

229 Cell line-specific pie charts built for the miRNA-mRNA interactions per mRNAs were similar.
230 Nevertheless, comparison of the most regulated sets of genes with 9 or more interactions each
231 revealed that these sets were cell-line-specific, with only 18 genes in common. These common
232 eighteen genes formed in average of 15.7+/-3.2 and 14.1+/- 2.4 interactions with microRNAs in the
233 HEK293 and Huh7.5 cell lines, respectively. Surprisingly, cell line-specific sets of microRNA
234 regulators for each of these genes were completely different. By PANTHER analysis of the common
235 set of genes, we detected enrichment in only one Gene Ontology (GO) category – a molecular
236 function of RNA binding (Supplementary Table 1).

237 Further, we identified a set of mRNAs capable of interaction with many different types of microRNA
238 molecules, with no preference to a particular miRNA. Such behavior of ambiguous interaction with
239 many microRNAs is similar to “sponge” performance of circular RNAs and lncRNAs. Among “sponge-
240 like” mRNAs with 50 or more interactions detected for each were *AGO1*, *EEF1A1* and *HSPA1B* in
241 HEK293/CLASH. Peculiarly, in Huh7.5/CLEAR-CLIP, same property attributed to different set of
242 mRNA, namely, *APOB*, *AFP*, *MALAT1* and *XIST*. In mRNAs with sponge-like property, microRNA
243 interaction sites were located predominantly in the protein coding part (Figure 2C and 2D).

244 Remarkably, in HEK293 cells, the most interacting mRNA was the one for AGO1 protein, which had
245 been overexpressed on purpose, as part of CLASH protocol. In this cell line, AGO1-encoding mRNA
246 has 88 interactions with a total of 50 different microRNAs. Mean expression levels for AGO1-binding
247 miRNAs were similar to that for all other miRNAs, at 7,279.36 counts vs 7,183.92 counts,
248 respectively. In addition to *AGO1* mRNA, HEK293 cell line expressed two other mRNAs displaying
249 non-specific sponge-like effect, *HSPA1B* with 77 interactions to 41 different microRNAs and *EEF1A1*
250 with 50 interactions to 42 microRNAs. Similar to artificially over-expressed AGO1mRNA, *EEF1A1* also
251 highly expressed in HEK293 cell line (>19K tpm), while another “sponge-like” mRNA *HSPA1B* had
252 expression level less than 1 tpm.

253 A set of “sponge-like” mRNAs expressed in Huh7.5 cell line was entirely different. There were two
254 protein-coding mRNAs, one for *AFP* - 47 interactions with 32 microRNAs and one for *APOB* - 47
255 interactions with 32 microRNAs, and two long-noncoding mRNAs, *MALAT1* with 47 interactions to
256 27 microRNAs and *XIST* with 55 interactions to 31 microRNAs. In coherence to expression levels of
257 “sponge-like” mRNAs in HEK293 cell line, we observed different expression level for these mRNAs:
258 *AFP* – more than 19K, *APOB* – 358 tpm, *XIST* – 202 tpm and *MALAT1* – 80 tpm, while the average
259 expression level in Huh7.5 was – 69 tpm.

260 **3.2.2 Comparative analysis of microRNA expression levels and their mRNA interacting properties**

261 To assess the role of microRNAs in the regulation of their target mRNAs, we studied two HEK293
262 and three Huh7.5 miRNA profiles retrieved from RNAseq datasets deposited in GEO (GSE75136 and
263 GSE74014). For each cell line, only high-quality datasets with very high correlation of miRNA-specific
264 expression levels were selected (Pearson’s correlation $r \gg 0.99$). For each miRNA, we analysed their
265 cell-line specific levels of expression by R package “DeSeq2” in order to normalize miRNA
266 expression, and compared these levels to the sets of experimentally detected microRNA-mRNA
267 interactions retrieved from HEK293/CLASH and Huh7.5/ CLEAR-CLIP datasets. MicroRNA was
268 considered as expressed if it had expression levels of more than 3 counts (see Methods). Less than a
269 quarter (23.5%) of 989 detected miRNAs was present in both cell lines (Figure 2E, Supplementary
270 Table 2). Notably, many microRNAs expressed in the HEK293 (N = 205) and Huh7.5 (N = 194) cell
271 lines then failed experimental detection as mRNA interacting molecules in CLASH or CLEAR-CLIP,
272 respectively.

273 On the other hand, both CLASH and CLEAR-CLIP datasets included many mRNA-interacting
274 microRNAs not detected in respective RNAseq datasets at all. On average, these microRNAs had
275 relatively small amounts of interactions: 2.2 ± 0.6 interacting partners for 197 microRNAs present
276 in CLASH dataset, but absent in HEK293-based RNAseq, and 5.1 ± 2.2 interacting partners for 168
277 miRNAs present in CLEAR-CLIP dataset but absent in Huh7.5-based RNAseq. For comparison, mean
278 amounts of detected interactions across all microRNAs were at 55.8 ± 12.7 for 398 miRNAs of
279 HEK293/CLASH and at 143.5 ± 28.5 for 542 miRNAs in Huh7.5/CLEAR-CLIP.

280 Next, for each of microRNAs we evaluated its cell-specific expression level and the amount of
281 interactions in this cell line (Supplementary Figure 2). For each cell line, Spearman correlations
282 levels were quite low, at 0.18 and 0.29 in HEK293 (N=335) and Huh7.5 (N=342), respectively. For
283 each miRNA, we calculated the cell line-specific ratios (R) of its expression level to amount of
284 detected interactions. The detailed analysis of this data allowed us to highlight two interesting types
285 of miRNA. Type 1 comprised microRNAs with high expression level and relatively small amount of
286 interactions with respective mRNAs. When the cut-offs for both R and expression levels were set as
287 ranking at 90th percentile or higher, only 16 miRNAs for HEK293 (expression > 4418 and ratio > 252)
288 and 12 miRNAs in Huh7.5 (expression > 6941 and ratio > 209) were classified as Type 1. Notably,
289 eight Type 1 miRNAs were present in both cell lines examined.

290 Type 2 microRNAs were characterized by a low R and many detected interactions with mRNAs.
291 When the cut-off for R was set as ranking at 10th percentile or lower, and amounts of interactions
292 at 90th percentile or higher, only 11 and 6 miRNAs for HEK293 (amount of interactions > 150 and
293 ratio < 0.9) and Huh7.5 (amount of interactions > 165 and ratio < 2.5), were classified as Type 2,
294 respectively. Unlike the Type 1 microRNAs, Type 2-specific sets from HEK293 and Huh7.5 did not
295 overlap.

296 In order to evaluate whether these types of microRNAs are evolutionarily constrained, for all
297 mature microRNAs from miRBase we calculated the mean of the phyloP conservative values in 20
298 vertebrates. The average cell line-specific phyloP scores for the Type 1 and Type 2 microRNAs were
299 similar, at 0.99 and 0.95, respectively. Notably, these scores were higher than the average score
300 value calculated for all known microRNAs (0.24) and the score values for all microRNAs that were
301 identified as expressed or interacted in HEK293 or Huh7.5 cell lines (0.74 and 0.71, respectively).
302 Notably, 80% of Top-100 miRbase microRNAs with the highest conservative phyloP scores were
303 seen either as expressed or interacted (or both) in at least one of these two cell lines. On average, in
304 HEK293 and Huh7.5 cells, these most conservative microRNAs had two times higher expression
305 levels than less conservative expressed microRNAs (Supplementary Table 2). Overall, higher than
306 average conservativeness of Type 1 and Type 2 microRNAs may point at the relative importance of
307 their functions.

308 **3.2.3 Comparing cellular contexts for microRNA's interactions**

309 As expected, a majority of microRNAs were concordant in two cell lines: their expression levels and
310 amounts of mRNA interactions were similar in both cellular contexts (Supplementary Figure 3A).
311 Nevertheless, some miRNAs have demonstrated remarkable cell specificity in their ratios R
312 (Supplementary Figure 3BC).

313 For 30 microRNAs, we detected high concordance between their expression level and amount of
314 experimentally detected interactions. Eighteen of these miRNAs had higher expression and mRNA
315 binding activity in Huh7.5 cell line, while for 12 remaining microRNA, both mRNA binding activity
316 and expression level were higher in HEK293 cells (Supplementary Figure 3B). As an example, in

317 Huh7.5 cell line, expression levels of MAPK1-repressing hsa-miR-194-5p (Kong et al., 2018) were 89
318 times higher than that in HEK293 cells; in Huh7.5 cells, this microRNA displayed 336 interactions,
319 while in HEK293 it formed only 7 interactions. On the other hand, in HEK293, expression levels of
320 lanosterol synthase suppressing hsa-miR-10a-5p (Kim et al., 2018) were 450 times higher than that
321 in Huh7.5 cells; in HEK293 cells, this microRNA displayed 267 interactions, while in Huh7.5 it formed
322 only 8 interactions. Such observations were expectable: microRNAs with higher expression level
323 may be capable of the binding to a larger repertoire of targets.

324 Peculiarly, a total of microRNAs have performed in exactly opposite way: in cells with higher
325 expression levels, these microRNAs displayed lesser amounts of interactions with their mRNA
326 targets (Supplementary Figure 3C). For example, in Huh7.5 cell line, expression levels of hsa-miR-
327 331-3p and hsa-miR-100-5p were at 1030 and 916 counts, respectively, while in HEK293 these
328 miRNAs had 65 and 41 expression counts, respectively. However, in both cases, amounts of
329 interactions in Huh7.5 cell line were lesser than that in HEK293 cell line, 47 versus 342 partners for
330 hsa-miR-331-3p, and 1 versus 30 partners for hsa-miR-100-5p. To investigate if this phenomenon is
331 due to the difference in the cell-specific expression levels of target genes, we performed an analysis
332 of all these targets. This was, as well, not the case. As an example, only 21 out of 318 individual
333 miRNA targets of hsa-miR-331-3p, were active in HEK293 cell line, but not detected in Huh7.5.

334 **3.3 Analysis of expanded set of experimentally confirmed microRNA binding regions**

335 Experimentally identified microRNA binding regions form a promising basis for further queries into
336 the basics of the gene expression regulation, and lead to uncovering novel disease-causing
337 mechanisms. To enhance a set of microRNA-mRNA interactions retrieved from CLASH and CLEAR-
338 CLIP studies, we performed the database integration of the data collected in cross-linking with
339 immunoprecipitation (CLIP) experiments that provide information about microRNA binding regions
340 of target genes, but unable to identify mRNA-microRNAs pairings.

341 For this purpose, we collected data from 79 CLIP experiments, comprising 61 HITS-CLIP and 18 PAR-
342 CLIP datasets covering 9 different cell lines, with a majority of these data obtained either in HEK293
343 (N=34 datasets) or Huh7.5 (N=19 datasets) cell lines (Supplementary Table 3). After combining CLIP
344 datasets with the data of previously mentioned CLASH and CLEAR-CLIP studies, approximately
345 156,000 unique microRNA binding regions catalogued within mRNA targets.

346 At the next stage, the set of microRNA binding regions was cleaned up to include only these
347 satisfying following criteria: (i) every position in this microRNA-binding subsequence is supported by
348 evidence from at least two different datasets or two different chimeric sequences and (ii) the length
349 of at least 10nt (Figure 3A, Supplementary Table 4). MiRNA-binding subsequences of this kind (N =
350 46,805) formed a dataset of experimentally confirmed microRNA binding regions (Exp-MiBR). In this
351 dataset, each Exp-MiBR record includes following attributes: genomic coordinates, gene name, type
352 of mRNA part, list of GEO GSM IDs for experiments which support this microRNA interaction,
353 cellular context, and the list of interacting microRNAs (if accessible). The criteria for inclusion of

354 individual microRNA-binding regions in Exp-MiBR database are justified by analysis presented in
355 Supplementary Table 5.

356 Exp-MiBR subsequences (N = 46,805) were mapped to approximately 15,000 human genes. About
357 one-half of Exp-MiBRs (48%) were located in 3'UTRs, 24% in a coding part, 10% in introns and 6% in
358 intergenic parts. Remaining 10% of the Exp-MiBRs were mapped to non-coding RNAs, being
359 matched to either exonic or intronic regions of these loci.

360 Approximately 68% of Exp-MiBRs were 20-40 nt in size, closely matching the mean length (33 nt) for
361 all input miRNA-binding regions from CLIPs, CLASH and CLEAR-CLIP data (Figure 3B). The second
362 peak in size distribution of Exp-MiBRs was at 75 to 80 nt, being predominantly comprised (86%) of
363 miRNA-interacting region extracted from CLEAR-CLIP dataset. While the sizes of 99% of the Exp-
364 MiBRs were smaller than 150nt, a few Exp-MiBRs were much longer than that, while remaining
365 supported by many experiments. The longest Exp-MiBR of 631 nt was formed by the regions
366 confirmed as microRNA-interacting in 54 different experiments in nine different cell lines. In
367 addition, there were a few Exp-MiBRs located closely to each other. Such clusters of Exp-MiBRs with
368 many interacting microRNAs do not display a tendency to any particular region of mRNA, as they
369 may be present in CDS, 3'UTR, 5'UTR or intergenic regions. As an example, chromosome 2 contains
370 a cluster of Exp-MiBRs covering an area of approximately 1.5 kb in size, which is located between
371 the loci of RNA5-8SP5 and MIR663B genes. According to CLASH and CLEAR-CLIP studies, this cluster
372 of Exp-MiBRs interacts with 52 different miRNAs (Supplementary Figure 4, Supplementary Table 6).

373 **3.4 Tissue-specific and housekeeping microRNA binding regions**

374 To characterize Exp-MiBRs further, we analyzed their tissue specificity. Most CLIP experiments were
375 performed either in HEK293 (43%) or in Huh7.5 (24%) cells, while the rest of the CLIP data were
376 collected in HeLa, HFF, BC-1, BC-3, EF3D, LCL35 or LCL cells. In HEK293 cells, we found
377 approximately 9,900 unique MiBRs, while analysis of Huh7.5 cells yielded 690 tissue-specific
378 interacting regions (Figure 3C). Larger amounts of Exp-MiBRs in HEK293 as compared to that Huh7.5
379 cells may be explained either by better coverage of HEK293 transcriptome by various CLIPs
380 (Supplementary Table3), or by intrinsic cell-specific features of miRNA interactomes.

381 Interestingly, some Exp-MiBRs were observed a majority of studied cells, possibly reflecting a
382 housekeeping function of these interactions. Approximately 1% of all Exp-MiBRs were found in
383 seven or more cell lines. The functional roles of 351 ubiquitous Exp-MiBRs were investigated using
384 Panther software. The GO analysis showed enrichment of genes participating in cellular process of
385 cell cycle (FC 3.17; p-value $1e-10-8$) and in molecular function of nucleic acid binding (FC 1.75; p-
386 value $5e-10-4$).

387 **3.5 Mitochondrial regulation by microRNA**

388 An analysis of Exp-MiBRs revealed that these microRNA interacting sequences cover 86% of the
389 mitochondrial genome, including 35 out of 37 mitochondrial genes. Mitochondrial Exp-MiBRs (N =
390 37) were found in all nine investigated cell lines, with each Exp-MiBR discovered, on average, in 11
391 independent experiments. In total, we identified 182 miRNAs that bound various mitochondrial
392 RNAs, with two mitochondrial regions binding 107 out of 182 miRNAs.

393

394 **4 Discussion**

395 Experimental identification of microRNA binding regions is an important prerequisite for querying
396 into the basics of the gene expression regulation, and for uncovering novel disease-causing
397 mechanisms. To date, only two sequencing-based experimental datasets describing full miRNA-
398 mRNA interactomes of human cells, CLASH and CLEAR-CLIP, are available. In both studies, the
399 primary goal was to develop and optimize the experimental protocol itself, while identifying miRNA-
400 mRNA interactions in a particular cell line grown under different conditions. Although these
401 techniques provide unique window into miRNA targeting, they are not free of limitations, which
402 precludes determining of entire miRNA-mRNA interactome. Nevertheless, intersecting CLASH and
403 CLEAR-CLIP datasets allowed us to detect much larger set of validated interactions than may be
404 expected of two randomly-generated datasets.

405 Typically, miRNA-mRNA interaction networks built in silico with an aid of one or another miRNA
406 prediction tool include thousands of mRNA targets. In our study, we attempted to paint a holistic
407 picture of human miRNA-mRNA interactome by comparing the entries from experimentally
408 collected datasets describing miRNA binding activity to the data describing expression data.
409 Interestingly, we found that more than half of mRNA transcripts do not bind to any miRNAs present
410 in the same cellular environment, while 1-2% of human transcripts interact with nine or more
411 miRNAs, thus, displaying a similar to sponge-like activity (Thomson and Dinger, 2016). Remarkably,
412 miRNA-mRNA sponge-like interactions were cell-lines specific, with very little overlap identified. In
413 HEK293 cells, the most prominent sponge-like activity resultant in 77 different miRNA interactions
414 was detected for *AGO1* mRNA, which had been initially overexpressed according to the CLASH
415 protocol. Two other “sponge-like” mRNAs *HSPA1B* and *EEF1A1* in HEK293 cell line formed 77 and 50
416 interactions respectively.

417 This amount of interactions is comparable to that of a well-known circular RNA with sponge
418 properties, *Cdr1as* (74 predicted sites) (Xu et al., 2015). In Huh7.5 cells, the set of RNAs with
419 “sponge-like” activities included many noncoding RNAs, including *MALAT1* and *XIST*. It is peculiar
420 that some Huh7.5-specific sponge-like RNAs, including these for alpha-fetoprotein (*AFP*) (Parpart et
421 al., 2014) and *APOB* (Bi et al., 2014) were previously described as biomarkers of liver carcinoma, a
422 tissue of origin for Huh7.5 cell line.

423 Some miRNAs expressed at relatively high levels were not among RNA interactors at all. About a
424 hundred of such non-interacting miRNAs were present in both studied cell lines. There is a
425 possibility that the natural targets for these microRNAs are either not expressed in studied cellular
426 contexts, or that they have no targets at all. In total, only 232 microRNAs had at least one
427 interaction in each of studied cell lines.

428 For individual miRNAs, levels of their expression have no bearing on amounts of interactions they
429 display, possibly reflecting difference in their functions depending on the cellular context. As an
430 example, we revealed that, in Huh7.5 cell line, miR-423-3p is abundant but displays only a few
431 interactions, while in HEK293 cell line the same miRNA forms more than two hundred interactions
432 and expressed at the quite low level. These observations complement previous findings of
433 Mullokandov and colleagues (Mullokandov et al., 2012), who have shown that the binding activity
434 of some highly expressed miRNAs may be weakened by either high target-to-miRNA ratio or the
435 relocation of this miRNA to the nucleus. Future studies are required for to investigate how RNA
436 binding properties of individual miRNAs may change in response to regulation by context-
437 dependent extrinsic or intrinsic factors.

438 Augmenting CLASH and CLEAR-CLIP datasets with additional 79 CLIP datasets provided us
439 with information about microRNA footprints resulted in many thousands of experimentally
440 confirmed microRNA binding regions (Exp-MiBR) present in both coding and noncoding regions of
441 RNA loci. At least some Exp-MiBR are tissue-specific, in agreement with Clark and colleagues, who
442 revealed the differences in the microRNA targetomes across tissues (Clark et al., 2014).

443 In addition to chromosomes, many Exp-MiBRs map to mitochondrial DNA, where they are quite
444 abundant. Previous studies showed four mitochondrial regions with high degree of homology to
445 microRNAs, namely, hsa-miR-4461 (chrM: 10690–10712), hsa-miR-4463 (chrM: 13050–13068), hsa-
446 miR-4484 (chrM: 5749–5766) and hsa-miR-4485 (chrM: 2562–2582) (Sripada et al., 2012). Two of
447 these regions, that encode mitochondrial *ND4L* and 16S rRNA genes, were also highly interacting
448 Exp-MiBRs, with 70 and 63 cognate miRNAs, respectively, all confirmed in nine different cell lines. In
449 both cases, previously identified cognate miRNAs hsa-miR-4461 and hsa-miR-4485 were among
450 confirmed interactors. Our study expands the coverage of mitochondrial genome by various miRNA-
451 interacting regions to 86% of its lengths. Altogether, these findings support the notion that miRNA-
452 mRNA interactions take place in a variety of cellular compartments, including mitochondria (Ni and
453 Leng, 2015).

454 Analysis of the landscape of microRNA-mRNA human interactions, which we derived from both
455 direct microRNA-mRNA interactions experimentally defined in HEK293 and Huh7.5 cell lines, along
456 with microRNA and mRNA expression data highlight complexity of human microRNA-mRNA
457 interactome. For individual miRNAs, levels of their expression have no bearing on amounts of
458 interactions they display, possibly reflecting difference in their functions depending on the cellular
459 context. In this article, we found that while only 1-2% of human genes were the most regulated by

460 microRNAs, a few cell line specific RNAs display a similar to sponge effect: *EEF1A1* and *HSPA1B* in
461 HEK293 and *AFP*, *APOB* and *MALAT1* genes in Huh7.5 cell lines. Some miRNAs might be expressed at
462 relatively low levels, and interact with many mRNAs. On the other hand, there is a set of microRNAs
463 expressed at a very high level and interacting with only a few mRNAs, thus, indeed, regulating
464 expression of their targets in a specific manner. Notably, microRNAs are capable of switching
465 between these two modes of action, depending on cellular context. The question of the biological
466 significance of these two miRNA groups is still open. CLASH and/or CLEAR-CLIP coverage of
467 additional cell lines is warranted. It is notable, however, that the presence of miRNA groups, one
468 with a low expression level and a high number of interactions, and one with opposite
469 characteristics, was detected in both cell lines profiled.

470 We have also established a collection of reliable microRNA binding regions that we systematically
471 extracted in course of analysis of 79 CLIP datasets, which is available at
472 <http://score.generesearch.ru/services/mirna/>. The promise of microRNAs as potential means for
473 diagnostics and therapy got expanded with a number of loss-of-function and, recently, the case of
474 disease-causing gain-of-function mutation in particular microRNA (Grigelioniene et al., 2019). We
475 believe that the results of our efforts in mapping the human miRNA-mRNA interactome may be
476 useful in untangling molecular underpinnings of hereditary and acquired diseases that involve
477 interactions.

478

479 **5 Conflict of Interest**

480 The authors declare that the research was conducted in the absence of any commercial or financial
481 relationships that could be construed as a potential conflict of interest.

482

483 **6 Author Contributions**

484 MS and OP designed the study and carried out the research. AB contributed to the discussion of the
485 results. OP and AB wrote the paper. All authors read and approved the final manuscript.

486

487 **7 Funding**

488 Not applicable.

489

490 **8 List of abbreviations**

491 AGO – Argonaute
492 CDS - Coding DNA sequence
493 CLASH – Crosslinking, ligation and sequencing of hybrids technique
494 CLEAR-CLIP - covalent ligation of endogenous Argonaute-bound RNA-CLIP technique
495 CLIP – UV crosslinking and immunoprecipitation technique
496 Exp-MiBRs - experimentally confirmed microRNA binding regions
497 HITS-CLIP – High-throughput sequencing of RNA isolated by crosslinking immunoprecipitation
498 iCLIP – individual-nucleotide resolution Cross-Linking and ImmunoPrecipitation
499 PAR-CLIP – Photoactivatable-Ribonucleoside-Enhanced Immunoprecipitation
500 UTR - Untranslated region

501

502 **9 Acknowledgments**

503 We thank Andrey Marakhonov and members of the Skoblov laboratory for helpful discussions.

504

505 **10 References**

- 506 Agarwal, V., Bell, G. W., Nam, J. W., Bartel, D. P. (2015). Predicting effective microRNA target sites in
507 mammalian mRNAs. *Elife*. 4 doi: 10.7554/eLife.05005.
- 508 Artcibasova, A. V., Korzinkin, M. B., Sorokin, M. I., Shegay, P. V., Zhavoronkov, A. A., Gaifullin, N., et
509 al. (2016). MiRImpact, a new bioinformatic method using complete microRNA expression profiles to
510 assess their overall influence on the activity of intracellular molecular pathways. *Cell Cycle*. 15(5),
511 689-698. doi: 10.1080/15384101.2016.1147633.
- 512 Bandiera, S., Pernot, S., El Saghire, H., Durand, S. C., Thumann, C., Crouchet, E., et al. (2016).
513 Hepatitis C Virus-Induced Upregulation of MicroRNA miR-146a-5p in Hepatocytes Promotes Viral
514 Infection and Deregulates Metabolic Pathways Associated with Liver Disease Pathogenesis. *J. Virol*.
515 90(14), 6387-6400. doi: 10.1128/JVI.00619-16.
- 516 Bartel, DP. (2004). MicroRNAs: genomics, biogenesis, mechanism, and function. *Cell*. 116(2), 281-97.

- 517 Bi, Y., He, Y., Huang, J., Su, Y., Zhu, G. H., Wang, Y., et al. (2014). Functional characteristics of
518 reversibly immortalized hepatic progenitor cells derived from mouse embryonic liver. *Cell. Physiol.*
519 *Biochem.* 34(4), 1318-38. doi: 10.1159/000366340.
- 520 Bray, N. L., Pimentel, H., Melsted, P., Pachter, L. (2016). Near-optimal probabilistic RNA-seq
521 quantification. *Nat. Biotechnol.* 34(5), 525-7. doi: 10.1038/nbt.3519.
- 522 Clark, P. M., Loher, P., Quann, K., Brody, J., Londin, E. R., Rigoutsos, I. (2014). Argonaute CLIP-Seq
523 reveals miRNA targetome diversity across tissue types. *Sci Rep.* 4, 5947. doi: 10.1038/srep05947.
- 524 Corcoran, D. L., Georgiev, S., Mukherjee, N., Gottwein, E., Skalsky, R. L., Keene, J. D., et al. (2011).
525 PARalyzer: definition of RNA binding sites from PAR-CLIP short-read sequence data. *Genome Biol.*
526 12(8), R79. doi: 10.1186/gb-2011-12-8-r79.
- 527 Friedman, R. C., Farh, K. K. H., Burge, C. B., Bartel, D. P. (2009). Most mammalian mRNAs are
528 conserved targets of microRNAs. *Genome Res.* 19(1), 92-105. doi: 10.1101/gr.082701.108.
- 529 Grigelioniene, G., Suzuki, H. I., Taylan, F., Mirzamohammadi, F., Borochowitz, Z. U., Ayturk, U. M., et
530 al. (2019). Gain-of-function mutation of microRNA-140 in human skeletal dysplasia. *Nature*
531 *medicine.* 1. doi: 10.1038/s41591-019-0353-2.
- 532 Grimson, A., Farh, K. K. H., Johnston, W. K., Garrett-Engele, P., Lim, L. P., Bartel, D. P. (2007).
533 MicroRNA targeting specificity in mammals: determinants beyond seed pairing. *Mol. Cell.* 27(1), 91-
534 105. doi: 10.1016/j.molcel.2007.06.017.
- 535 Gumienny, R, and Zavolan, M. (2015). Accurate transcriptome-wide prediction of microRNA targets
536 and small interfering RNA off-targets with MIRZA-G. *Nucleic Acids Res.* 43(3), 1380-91. doi:
537 10.1093/nar/gkv050.
- 538 He, L, and Hannon, GJ. (2004). MicroRNAs: small RNAs with a big role in gene regulation. *Nat. Rev.*
539 *Genet.* 5(7), 522-31. doi: 10.1038/nrg1379.
- 540 Heberle, H., Meirelles, G. V., da Silva, F. R., Telles, G. P., Minghim, R. (2015). InteractiVenn: a web-
541 based tool for the analysis of sets through Venn diagrams. *BMC Bioinformatics.* 16, 169. doi:
542 10.1186/s12859-015-0611-3.
- 543 Helwak, A., Kudla, G., Dudnakova, T., Tollervey, D. (2013). Mapping the human miRNA interactome
544 by CLASH reveals frequent noncanonical binding. *Cell.* 153(3), 654-65. doi:
545 10.1016/j.cell.2013.03.043.
- 546 Hu, B., Yang, Y. C. T., Huang, Y., Zhu, Y., Lu, Z. J. (2016). POSTAR: a platform for exploring post-
547 transcriptional regulation coordinated by RNA-binding proteins. *Nucleic Acids Res.* 45(D1), D104-
548 D114. doi: 10.1093/nar/gkw888.

- 549 Jonas, S, and Izaurralde, E. (2015). Towards a molecular understanding of microRNA-mediated gene
550 silencing. *Nat. Rev. Genet.* 16(7), 421-33. doi: 10.1038/nrg3965.
- 551 Karolchik, D., Hinrichs, A. S., Furey, T. S., Roskin, K. M., Sugnet, C. W., Haussler, D., et al. (2004). The
552 UCSC Table Browser data retrieval tool. *Nucleic Acids Res.* 32(Database issue), D493-6. doi:
553 10.1093/nar/gkh103.
- 554 Kim, J. E., Hong, J. W., Lee, H. S., Kim, W., Lim, J., Cho, Y. S., et al. (2018). Hsa-miR-10a-5p
555 downregulation in mutant UQCRB-expressing cells promotes the cholesterol biosynthesis pathway.
556 *Sci Rep.* 8(1), 12407. doi: 10.1038/s41598-018-30530-6.
- 557 Kong, Q., Zhang, S., Liang, C., Zhang, Y., Kong, Q., Chen, S., et al. (2018). LncRNA XIST functions as a
558 molecular sponge of miR-194-5p to regulate MAPK1 expression in hepatocellular carcinoma cell. *J.*
559 *Cell. Biochem.* 119(6), 4458-4468. doi: 10.1002/jcb.26540.
- 560 Kozomara, A, and Griffiths-Jones, S. (2014). miRBase: annotating high confidence microRNAs using
561 deep sequencing data. *Nucleic Acids Res.* 42(Database issue), D68-73. doi: 10.1093/nar/gkt1181.
- 562 Li, Y., and Zhang, Z. (2014). Potential microRNA-mediated oncogenic intercellular communication
563 revealed by pan-cancer analysis. *Scientific reports.* 4, 7097. doi: 10.1038/srep07097.
- 564 Li, Y., Liang, C., Wong, K. C., Jin, K., Zhang, Z. (2014). Inferring probabilistic miRNA-mRNA interaction
565 signatures in cancers: a role-switch approach. *Nucleic acids research.* 42(9), e76-e76. doi:
566 10.1093/nar/gku182.
- 567 Licatalosi, D. D., Mele, A., Fak, J. J., Ule, J., Kayikci, M., Chi, S. W., et al. (2008). HITS-CLIP yields
568 genome-wide insights into brain alternative RNA processing. *Nature.* 456(7221), 464-9. doi:
569 10.1038/nature07488.
- 570 Lu, Y, and Leslie, CS. (2016). Learning to Predict miRNA-mRNA Interactions from AGO CLIP
571 Sequencing and CLASH Data. *PLoS Comput. Biol.* 12(7), e1005026. doi:
572 10.1371/journal.pcbi.1005026.
- 573 Luna, J. M., Scheel, T. K., Danino, T., Shaw, K. S., Mele, A., Fak, J. J., et al. (2015). Hepatitis C virus
574 RNA functionally sequesters miR-122. *Cell.* 160(6), 1099-110. doi: 10.1016/j.cell.2015.02.025.
- 575 Moore, M. J., Scheel, T. K., Luna, J. M., Park, C. Y., Fak, J. J., Nishiuchi, E., et al. (2015). miRNA-target
576 chimeras reveal miRNA 3'-end pairing as a major determinant of Argonaute target specificity. *Nat*
577 *Commun.* 6, 8864. doi: 10.1038/ncomms9864.
- 578 Moore, M. J., Zhang, C., Gantman, E. C., Mele, A., Darnell, J. C., Darnell, R. B. (2014). Mapping
579 Argonaute and conventional RNA-binding protein interactions with RNA at single-nucleotide

- 580 resolution using HITS-CLIP and CIMS analysis. *Nat Protoc.* 9(2), 263-93. doi:
581 10.1038/nprot.2014.012.
- 582 Mullokandov, G., Baccharini, A., Ruzo, A., Jayaprakash, A. D., Tung, N., Israelow, B., et al. (2012).
583 High-throughput assessment of microRNA activity and function using microRNA sensor and decoy
584 libraries. *Nat. Methods.* 9(8), 840-6. doi: 10.1038/nmeth.2078.
- 585 Murakawa, Y., Hinz, M., Mothes, J., Schuetz, A., Uhl, M., Wyler, E., et al. (2015). RC3H1 post-
586 transcriptionally regulates A20 mRNA and modulates the activity of the IKK/NF- κ B pathway. *Nat*
587 *Commun.* 6, 7367. doi: 10.1038/ncomms8367.
- 588 Ni, WJ, and Leng, XM. (2015). Dynamic miRNA-mRNA paradigms: New faces of miRNAs. *Biochem*
589 *Biophys Rep.* 4, 337-341. doi: 10.1016/j.bbrep.2015.10.011.
- 590 Parpart, S., Roessler, S., Dong, F., Rao, V., Takai, A., Ji, J., et al. (2014). Modulation of miR-29
591 expression by α -fetoprotein is linked to the hepatocellular carcinoma epigenome. *Hepatology.*
592 60(3), 872-83. doi: 10.1002/hep.27200.
- 593 Plotnikova, OM, and Skoblov, MY. (2018). Efficiency of the miRNA- mRNA Interaction Prediction
594 Programs. *Mol. Biol. (Mosk.).* 52(3), 543-554. doi: 10.7868/S0026898418030187.
- 595 Riffo-Campos, Á., Riquelme, I., Brebi-Mieville, P. (2016). Tools for Sequence-Based miRNA Target
596 Prediction: What to Choose?. *Int J Mol Sci.* 17(12) doi: 10.3390/ijms17121987.
- 597 Sætrom, P., Heale, B. S., Snøve Jr, O., Aagaard, L., Alluin, J., Rossi, J. J. (2007). Distance constraints
598 between microRNA target sites dictate efficacy and cooperativity. *Nucleic Acids Res.* 35(7), 2333-42.
599 doi: 10.1093/nar/gkm133.
- 600 Selbach, M., Schwanhäusser, B., Thierfelder, N., Fang, Z., Khanin, R., Rajewsky, N. (2008).
601 Widespread changes in protein synthesis induced by microRNAs. *Nature.* 455(7209)6 58-63. doi:
602 10.1038/nature07228.
- 603 Sripada, L., Tomar, D., Prajapati, P., Singh, R., Singh, A. K., Singh, R. (2012). Systematic analysis of
604 small RNAs associated with human mitochondria by deep sequencing: detailed analysis of
605 mitochondrial associated miRNA. *PLoS ONE.* 7(9), e44873. doi: 10.1371/journal.pone.0044873.
- 606 Steinkraus, B. R., Toegel, M., Fulga, T. A. (2016). Tiny giants of gene regulation: experimental
607 strategies for microRNA functional studies. *Wiley Interdiscip Rev Dev Biol.* 5(3), 311-62. doi:
608 10.1002/wdev.223.
- 609 Thomson, DW, and Dinger, ME. (2016). Endogenous microRNA sponges: evidence and controversy.
610 *Nat. Rev. Genet.* 17(5), 272-83. doi: 10.1038/nrg.2016.20.

- 611 Uhlmann, S., Mannsperger, H., Zhang, J. D., Horvat, E. Á., Schmidt, C., Küblbeck, M., et al. (2012).
612 Global microRNA level regulation of EGFR-driven cell-cycle protein network in breast cancer. *Mol.*
613 *Syst. Biol.* 86 570. doi: 10.1038/msb.2011.100.
- 614 Wang, K., Li, M., Hakonarson, H. (2010). ANNOVAR: functional annotation of genetic variants from
615 high-throughput sequencing data. *Nucleic Acids Res.* 38(16), e164. doi: 10.1093/nar/gkq603.
- 616 Weiss, CN, and Ito, K. (2017). A Macro View of MicroRNAs: The Discovery of MicroRNAs and Their
617 Role in Hematopoiesis and Hematologic Disease. *Int Rev Cell Mol Biol.* 334, 99-175. doi:
618 10.1016/bs.ircmb.2017.03.007.
- 619 Wissink, E. M., Fogarty, E. A., Grimson, A. (2016). High-throughput discovery of post-transcriptional
620 cis-regulatory elements. *BMC Genomics.* 17, 177. doi: 10.1186/s12864-016-2479-7.
- 621 Xu, H., Guo, S., Li, W., Yu, P. (2015). The circular RNA Cdr1as, via miR-7 and its targets, regulates
622 insulin transcription and secretion in islet cells. *Sci Rep.* 5, 12453. doi: 10.1038/srep12453.
- 623 Yang, H, and Wang, K. (2015). Genomic variant annotation and prioritization with ANNOVAR and
624 wANNOVAR. *Nat Protoc.* 10(10), 1556-66. doi: 10.1038/nprot.2015.105.

625

626 **11 Figure Caption**

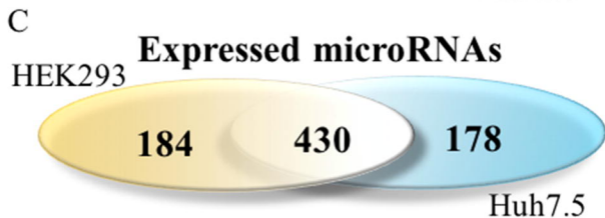
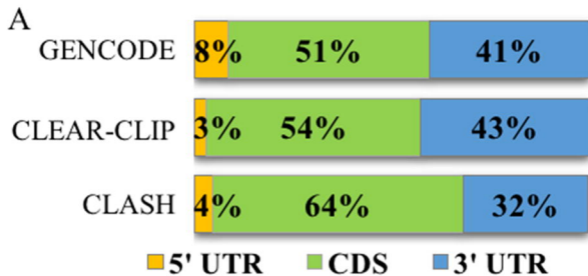
627 **Figure 1. A comparison of CLASH and CLEAR-CLIP datasets. (A)** Distribution of the summarized
628 lengths of 3'UTR, CDS or 5'UTR mRNA regions in CLEAR-CLIP, CLASH and GENCODE, respectively. **(B)**
629 Venn diagram of HEK293- and Huh7.5-expressed genes as covered by CLASH and CLEAR-CLIP
630 interactomes, respectively. **(C)** Venn diagram of HEK293- and Huh7.5-expressed miRNAs
631 represented in CLASH and CLEAR-CLIP interactomes, respectively.

632 **Figure 2. microRNA and mRNA expression analysis in HEK293 and Huh7.5 cell lines. (A) and (B):**
633 Analysis of expressed genes according to amounts of their interactions with microRNAs in HEK293
634 **(A)** and Huh7.5 **(B)** cell lines; **(C) and (D):** Locations of experimentally confirmed microRNA binding
635 regions (Exp-MiBRs) in sponge-like RNAs expressed in HEK293/CLASH **(C)** and Huh7.5/ CLEAR-CLIP
636 **(D)** datasets. After segmenting each of the presented RNAs into 50nt-pieces, the segments
637 coinciding with Exp-MiBR were marked blue on the mRNA map. For each sponge RNA, name and
638 length are above the gene schematics. Colored parts of RNAs are as follows: 5'UTR –yellow, coding
639 region – violet, 3'UTR – green, noncoding region – grey. **(E)** The overlaps between expressed and
640 interacting microRNAs in HEK293 and Huh7.5 cell lines.

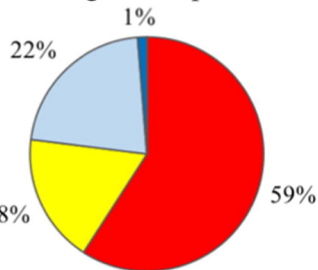
641 **Figure 3. The detailed analysis of experimentally confirmed microRNA binding regions (Exp-**
642 **MiBRs).** **(A)** Validation of the Exp-MiBR by their independent occurrence in two or more datasets, or
643 in two or more chimeric sequences from one dataset. **(B)** Exp-MiBRs: distribution of the lengths. On

644 horizontal axis – the length of the Exp-MiBRs subsequence; on vertical axis – amounts of the
645 detected Exp-MiBRs (N). **(C)** Venn diagram depicting tissue specificity of Exp-MiBRs detected in
646 HEK293, Huh7.5 and all other cell lines **(D)**. Venn diagram depicting Exp-MiBRs detected in
647 experiments employing three different types of identification techniques.

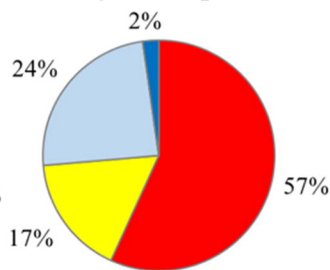
648



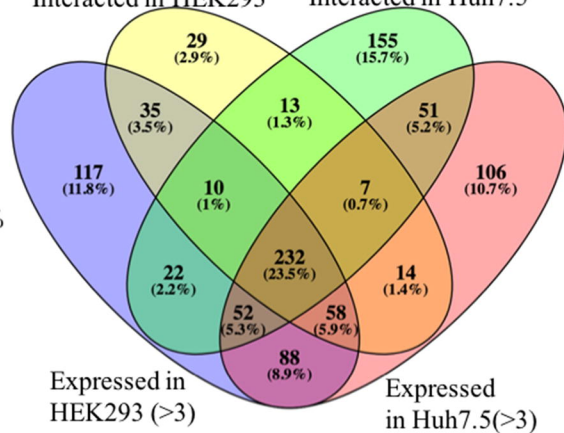
A HEK293
15.8k genes expressed



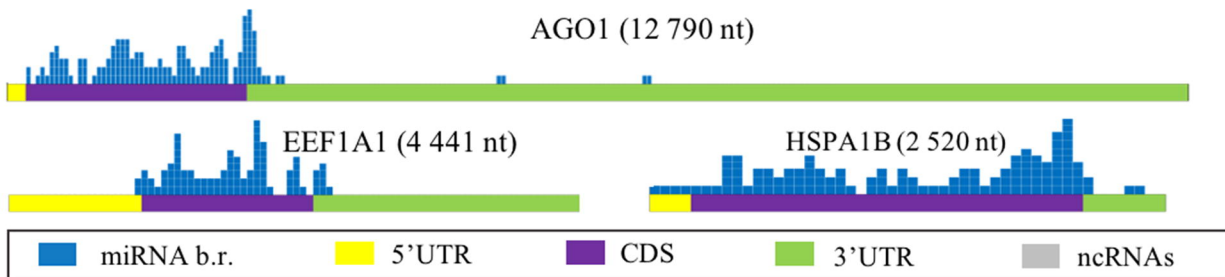
B Huh7.5
14.5k genes expressed



E Interacted in HEK293 Interacted in Huh7.5



C HEK293:



D Huh7.5:

